A TIME SPLITTING METHOD FOR EVOLUTION EQUATIONS MODELLING BENARD CONVECTION/

UM MÉTODO DE SEPARAÇÃO TEMPORAL DE VARIÁVEIS PARA EQUAÇÕES DE EVOLUÇÃO UTILIZADAS NA MODELAGEM DE CONVECÇÃO DE BENARD

J. Pontes
PEMM/COPPE/UFRJ
PO Box 68505, 21945–970 Rio de Janeiro, R. J. Brazil *jopontes@metalmat.ufrj.br*

C. I. Christov
National Intitute of Meteorology and Hydrology
66 Tsarigradsko Chaussee, Sofia 1784, Bulgaria *christov@meteo.bg*

Abstract

Pattern formation in a thin layer of fluid heated by below is often studied by numerical integration of nonlinear parabolic equations, containing fourth-order space-derivatives in the x and the y directions. A finite-difference semi-implicit coordinate-splitting scheme of first order in time and of second order in space is developed and applied to solving two such equations in finite geometries, namely the Swift-Hohenberg and the Knobloch equations. The construction of the scheme is accomplished by assigning terms to the implicit and to the explicit parts, and by replacing the spatial and time operators by discrete representations. The stability properties of the algorithm are defined at this stage. The scheme is splitted in two equivalent equations, to reduce the storage requirements. The resulting algebraic linear system displays a left hand side operator with a pentadiagonal structure and is solved by gaussian elimination with pivoting. Some results and a criteria to characterize the asymptotic state are presented.

Keywords

Nonlinear Systems, Bénard Convection, Implicit Methods, Finite Difference Methods
Sistemas não-lineares, Convecção de Bénard, Métodos Implícitos, Método de diferenças finitas

1 INTRODUCTION

We present a finite-difference semi-implicit coordinate-splitting scheme of first order in time and of second order in space developed to numerically solving time-evolution parabolic equations with fourth-order space derivatives. The scheme is applied to integrating two evolution equations used in the study of pattern formation in a thin layer of fluid with large Prandtl number, heated from below. The first equation was derived by Swift & Hohenberg (1977) and describes Rayleigh-Bénard convective patterns in layers confined between horizontally good-conducting boundaries. The second one was derived

by Knobloch (1990) and describes pattern formation in layers confined between horizontally poor-conducting boundaries, induced by buoyancy or by surface-tension instabilities.

In fluids with large Prandtl number, the response of the velocity field to changes in the system state is much faster than the response of the temperature field. The velocity field is *slave* of the temperature field. In consequence, the system evolution can be described in terms of a two-dimensional (x and y) function representing the average vertical deviation of the local temperature from the conductive state. The single dependent variable in the Swift-hohenberg and in the Knobloch equations represents that average deviation.

2 POSING THE PROBLEM

The condition of stability of explicit numerical schemes imposes, as a rule, very restrictive limitations on the time increment used in the numerical integration of evolution equations. It is much more true when the equations contain fourth-order derivatives, where $\tau \leq (\Delta x)^4/4$. Implicit schemes are not subjected to that limitation but the straightforward implementation in more than one spatial dimension results into very large linear systems. An effective way to combine the stability properties of implicit schemes and the storage-efficiency of the explicit ones is to use the so-called coordinate splitting. The time step is implemented through several *half-time steps* in which only one of the operators is implemented implicitly. The notion of splitting (Peaceman & Rachford, 1955, Douglas & Rachford, 1956) was introduced for the second-order parabolic equation (heat equation) and proved very fruitful (see Yanenko (1971), for a review of the earlier results).

To the best of our knowledge, coordinate splitting methods had not been applied to parabolic equations with higher-order diffusion operators (see also Christov *et al.*, 1997, Pontes *et al.*, 1996). In the present work we corroborate the technique of splitting with application to the Swift-Hohenberg and Knobloch equations. These equations are, respectively,

$$\tau_0 \frac{\partial u}{\partial t} = \varepsilon u - g u^3 - \xi^4 \left(\nabla^2 + \kappa_0^2\right)^2 u, \tag{1}$$

$$\begin{aligned} \tau_0 \frac{\partial u}{\partial t} &= \alpha u - \mu \nabla^2 u - \nabla^4 u + \\ &\quad \kappa \nabla \cdot |\nabla u|^2 \nabla u + \beta \nabla \cdot \nabla^2 u \nabla u - \gamma \nabla \cdot u \nabla u + \delta \nabla^2 |\nabla u|^2. \end{aligned} \tag{2}$$

Here, $u(x, y, t)$ is the horizontal planform of the temperature deviation from the conductive profile. The parameter κ_0 in Eq. (1) is the critical wavenumber of the structure. The coefficient μ in Eq. (2) is the scaled bifurcation parameter, and α represents the effect finite thermal conductivity of the horizontal boundaries, or finite Biot number. The coefficients β, δ and γ are present when the boundary conditions at top and bottom are not identical ($\beta \neq 0, \delta \neq 0$) or when non-Boussinesq effects are taken into account ($\gamma \neq 0$). The coefficient κ can always be scalled to ± 1 (Knobloch, 1990).

We rescale the space coordinates x and y as well as κ_0 in the Swift-Hohenberg equation by introducing the new variables $x^* = x/\xi$, $y^* = y/\xi$ and $\kappa^* = \kappa_0/\xi$. The time is also rescaled according to $\tau = t/\tau_0$. However we shall write the new variables without the asterisk in order to simplify the notation.

Boundary conditions are set to $u = \partial u/\partial n = 0$ at the sidewalls, where n is the direction of the unitary vector pependicular to the walls.

3 THE SPLITTING

First we show the desired form of the first-order in time implicit scheme for Eqs. (1, 2) in full time steps. According to the role of the different terms they are taken either on the "new" time step, $n+1$, or on the "old" one, n. Then, the implicit scheme reads:

$$\frac{u^{n+1}-u^n}{\tau} = \left(\Lambda_x^n + \Lambda_y^n\right) u^{n+1} + f^n, \tag{3}$$

whose equivalent form is as follows:

$$\left(I - \tau\,\Lambda_x^n + \Lambda_y^n\right) u^{n+1} = u^n + \tau\, f^n. \tag{4}$$

The main idea is to invert on the "new" time stage $n+1$ the negative definite operators in order to avoid the limitations on the time increment of the type $\tau \sim \mathcal{O}(\Delta x^4)$ while the non-definite lower-order operators are kept on the "old" time stage n. The operators Λ_x^n, Λ_y^n and the function f^n are defined by:

$$\Lambda_x^n = \frac{\partial^4}{\partial x^4} - \left(\frac{\kappa_0^4}{2} + \frac{3}{2}(u^n)^2\right), \tag{5}$$

$$\Lambda_y^n = \frac{\partial^4}{\partial y^4} - \left(\frac{\kappa_0^4}{2} + \frac{3}{2}(u^n)^2\right), \tag{6}$$

$$f^n = \varepsilon\, u^n + 2(u^n)^3 - 2\frac{\partial^4 u^n}{\partial x^2 \partial y^2} - 2\kappa_0^2\left(\frac{\partial^2}{\partial x^2} + \frac{\partial^2}{\partial y^2}\right) u^n, \tag{7}$$

in the case of the Swift-Hohenberg equation. The nonlinear term, gu^3, is evaluated in the "new" time stage $n+1$ according to $g(u^3)^{n+1} \approx 3(u^2)^n\, u^{n+1} - 2(u^3)^n$.

In the case of the Knobloch equation, Λ_x^n, Λ_y^n and f^n are defined by:

$$\Lambda_x^n = \frac{\alpha}{2} - \frac{\partial^4}{\partial x^4} + \kappa\frac{\partial}{\partial x}\left(|\nabla u^n|^2\,\frac{\partial}{\partial x}\right), \tag{8}$$

$$\Lambda_y^n = \frac{\alpha}{2} - \frac{\partial^4}{\partial y^4} + \kappa\frac{\partial}{\partial y}\left(|\nabla u^n|^2\,\frac{\partial}{\partial y}\right), \tag{9}$$

$$f^n = -2\frac{\partial^4 u^n}{\partial x^2 \partial y^2} - \mu\nabla^2 u^n + \beta\nabla\cdot\nabla^2 u^n \nabla u^n - \gamma\nabla\cdot u^n\nabla u^n + \delta\nabla^2|\nabla u^n|^2. \tag{10}$$

For the boundary conditions considered here, the mixed fourth derivative is an oblique operator and does not affect the stability, but is taken on the "new" time stage since it spoils the structures of the matrices to be inverted when the splitting is effected. For this reason it is left on the "old" time stage. Equation (4) results in a three-dimensional matrix of "stereo-five diagonal" structure. The inversion of this kind of matrix is an expensive procedure even though it is sparse. The most acceptable way to avoid this problem is to use coordinate splitting.

The first thing one can do here is to generalize the so-called *Alternating Directions Implicit (ADI)* scheme (Douglas & Rachford, 1956). However, ADI is at its stability margin and the inclusion of nonlinear terms could bring into play considerable limitations on the time increment. That is why we prefer the scheme of *Stabilizing Correction*, also called *Second Douglas Scheme* (Yanenko, 1971), which is more robust for nonlinear problems than ADI. Besides, Stabilizing Correction is stable in 3D while ADI is not even for linear problems. The only disadvantage is that the Second Douglas Scheme is first order in time. In terms of the notation of the present work, we have the following:

$$\frac{\tilde{u} - u^n}{\tau} = \Lambda_x^n \, \tilde{u} + \Lambda_y^n \, u^n + f^n, \tag{11}$$

$$\frac{u^{n+1} - \tilde{u}}{\tau} = \Lambda_y^n (u^{n+1} - u^n). \tag{12}$$

In order to show that the splitting scheme approximates the original implicit scheme we rewrite eqs. (11, 12) as follows:

$$(I - \tau \, \Lambda_x^n) \, \tilde{u} = \left(I + \tau \, \Lambda_y^n\right) u^n + \tau \, f^n, \tag{13}$$

$$\left(I - \tau \, \Lambda_y^n\right) u^{n+1} = \tilde{u} - \tau \, \Lambda_y^n \, u^n. \tag{14}$$

In order to exclude the intermediate variable $\tilde{u}$ we apply the operator $(I - \tau \, \Lambda_x^n)$ to Eq. (14) and add the result to Eq. (13), namely

$$(I - \tau \, \Lambda_x^n)(I - \tau \, \Lambda_y^n) u^{n+1} = (I + \tau \, \Lambda_y^n) u^n - \tau (I - \tau \, \Lambda_x^n) \Lambda_y^n \, u^n + \tau \, f^n, \tag{15}$$

or else,

$$\left(I - (\tau)^2 \; \Lambda_x^n \Lambda_y^n)\right) \frac{u^{n+1} - u^n}{\tau} = (\Lambda_x^n + \Lambda_y^n) u^{n+1} + f^n. \tag{16}$$

The latter is in fact Eq. (3) save the operator $B \equiv I + \tau^2 \Lambda_x^n \Lambda_y^n = I + \mathcal{O}(\tau^2)$, acting upon the time difference $(u^{n+1} - u^n)/\tau$. One sees that the time splitting scheme approximates the original scheme within the order $\mathcal{O}(\tau^2)$, which is better than the order of approximation of the latter. In other words, the splitting scheme coincides with the original scheme within the order of approximation of the latter.

When the norm of the operator B is greater than unit the splitting scheme is even more stable than the original one. In fact, the scheme proved to be stable for all time steps used in the tests performed with the Swift-Hohenberg code. In the case of Eq. (2), the operator acting on the unknowns is not always negative definite, so a limit for the time step used in the numerical simulations exists in certain regions of the parameters domain of that equation.

The implementation of the semi-implict scheme consists in defining a rectangular grid of points over the system and in solving Eqs. (13, 14) in the points of the grid, using the system state at each step n as the initial condition to evaluate u in the time $n + 1$. A random initial condition was assigned as the system state in $t = 0$.

Eq. (13) is decoupled from Eq. (14), being solved first in each time step n. Furthermore, the former contains space derivatives in x direction only. In consequence, the equation associated to each particular point of the grid is coupled to the equation of neighbour points in the same line, but not to equations associated to points of other lines. Eq. (11) is then solved line by line, reducing the storage requirements of the numerical code. A system of algebraic linear equations is obtaining for each line, where the operator acting in the vector of unknows diplays a penta-diagonal structure. First, all operators are evaluated and then, the linear system associated to each line is solved by gaussian elimination with pivoting.

Upon solving Eq. (13) we store the results concerning the operator $(I + \tau \, \Lambda_y^n)$ and $\tau \, \Lambda_y^n u^n$, which will be used to solve Eq. (14). So, at the end of the first "half-step", when Eq. (13) has been solved in all lines, all operators and known variables appearing in Eq. (14) have already been evaluated. The second "half-step" reduces to merely solving Eq. (14) column by column.

4 ASYMPTOTIC STATES

When performing the numerical simulations we faced the problem of distinguishing time-dependent and time-independent asymptotic states. In the latter case we needed a criteria to ascertaining when a pattern still evolved, and further qualitative changes were likely to occur, or rather, when we could, with reasonable confidence, expect that only minor adjustments would possibly occur, not justifying to proceed with the computational effort. In the case of the Swift-hohenberg equation the patterns always evolve towards time-independent asymptotic states, since that equation admits a Lyapunov potential in the form

$$\Psi = \tau_0 \int_D \left[-\frac{\varepsilon}{2} u^2 + \frac{g}{4} u^4 + \frac{\xi^4}{2} \left((\nabla^2 + \kappa_0^2) u \right)^2 \right] dx\, dy, \tag{17}$$

$$\frac{\partial \Psi}{\partial t} = -\tau_0 \int_D \left(\frac{\partial u}{\partial t} \right)^2 dx\, dy < 0. \tag{18}$$

The existence of a Lyapunov potential rules out possible time-dependent behavior in the long times. In the case of the Knobloch equation no such potential exits, opening to the possibility of existence of time-dependent asymptotic states. We found both time-dependent and time-indepent asymptotic patterns in our simulations of Eq. (2).

We followed the time evolution of patterns by monitoring a figure that measures the rate of change of the *distance* between two successive states of the system, and is sensitive to the evolution of both the *amplitude* and the *phase*. This figure is defined by (Christov *et. al.*, 1997), (Pontes *et. al.*, 1996):

$$L_1 = \frac{1}{\tau} \frac{\sum_{i,j} |u_{i,j}^{n+1} - u_{i,j}^n|}{\sum_{i,j} |u^{n+1}|}, \tag{19}$$

where the summs are made over the i and j points of the spatial grid. In the case of patterns that evolve towards an asymptotic steady state three different stages of evolution can be distinguished : In the first one, the velocity of evolution rapidly decays from a very high value. This is the stage in which the pattern forms, grows and the *amplitude* of the structure saturates under the action of the nonlinearities of the problem. However the pattern displays a high density of defects. In the second phase L_1 presents an irregular behaviour, but clearly non-decaying. Defects are eliminated, dislocations "climb" or "glide", the number of "grains" diminishes and the whole pattern moves. This is the stage in which the *phase* evolves. In the third stage no further qualitative changes are observed and the velocity of evolution L_1 exponentially decays. We suspended the numerical simulations after observing a sustained exponential decay of L_1.

In cases in which the system evolves towards a time-dependent pattern, L_1 initially decays, when the structure forms. Then it displays an irregular non-decaying behaviour at a level much higher than the one seen in patterns that evolve to a stady state.

5 NUMERICAL RESULTS

In this section we present some results obtained with two numerical codes based on the semi-implicit scheme above described. Fig. 1 shows a sequence of images obtained by integration of Eq. (1) and the associated $L_1 \times t$ curve. The bifurcation parameter ε varies linearly along the x direction from 0 to 0.2. A numerical grid containing 82×202

points was used, leading to a mesh of aproximately eight points per wavelength of the structure. The time-step used in the simulation was $\Delta t = 0.0085$, so approximately 10^6 time steps were accomplished in the simulation. The first image shows the random initial condition, and the following ones show an unstable focus, the colapse of the focus and the asymptotic time-independent pattern. The $L_1 \times t$ curve captures the acceleration of the dynamics when the focus colapses, and the decay of the rate of evolution, as the pattern approaches a steady state.

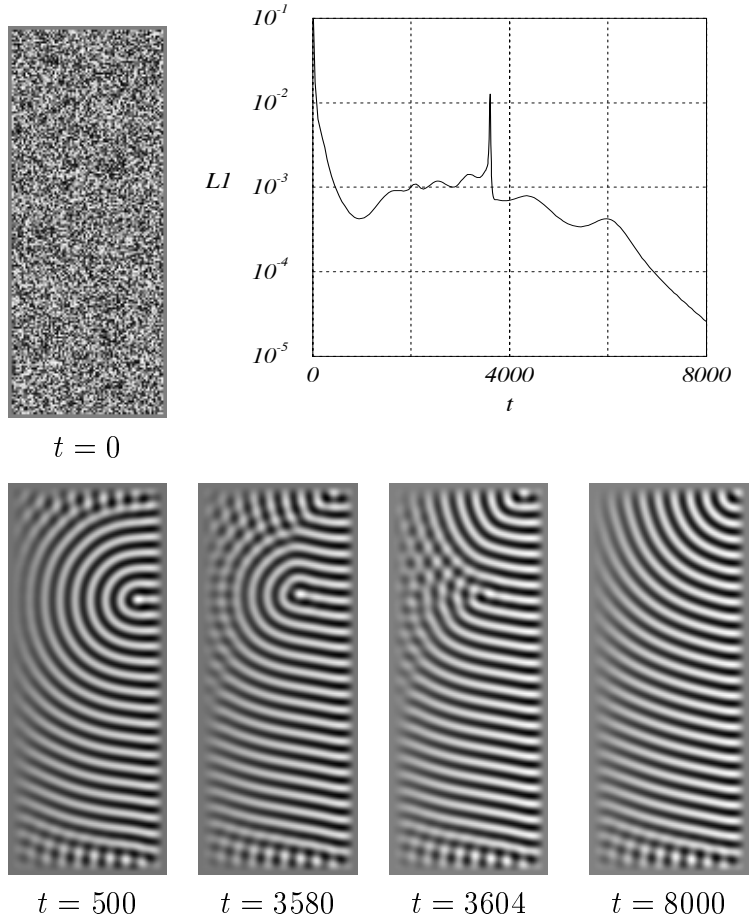

Figure 1: Evolution of a Bénard pattern obtained by integration of Eq. (1) with $\tau_0 = 0.0509$, $g = 1.29$, $\xi^4 = 0.015$, $\kappa_0 = 3.1172$ and ε linearly varying along x, from 0 to 0.2. The $L_1 \times t$ displays a sharp peak around $t = 3600$, when the focus appearing in $t = 500$ colapses. After that no further qualitative changes occur.

Figs. 2–4 show the results from integration of Eq. (2). The selected type of tesselation depends on the coefficients of the quadratic terms, β, γ and δ. Stable patterns include squares, hexagons, rolls and the coexistence of these motifs (Knobloch, 1990, Shtilman & Sivashinsky, 1991, Pontes *et. al.*, 1996) . Besides, this equation holds a non-variational structure, opening to the possibility of existence of time-dependent asymptotic patterns. Fig. 2 shows an evolution from the random initial condition to a time-independent tesselation of squares. A time step $\Delta t = 0.1$ was used in this simulation, so 2×10^6 of time-steps were accomplished. A numerical grid containing 402×402 points was used, leading to a mesh of aproximately 16 points per wavelenght of the pattern. All defects disappear before $t = 30000$, then the pattern slowly moves to align with the sidewalls.

Fig. 4 shows a time-dependent pattern, aperiodic in space and time. The numerical grid contains 202×202 points and a time-step $\Delta t = 5 \times 10^{-3}$ was used in this simulation.

6 CONCLUSIONS

The results presented in this work show that coordinate splitting schemes can be successefully implementeded to numerically solving parabolic equations containing fourth-order space-derivatives. These schemes are not subjected to the severe limitations on the time

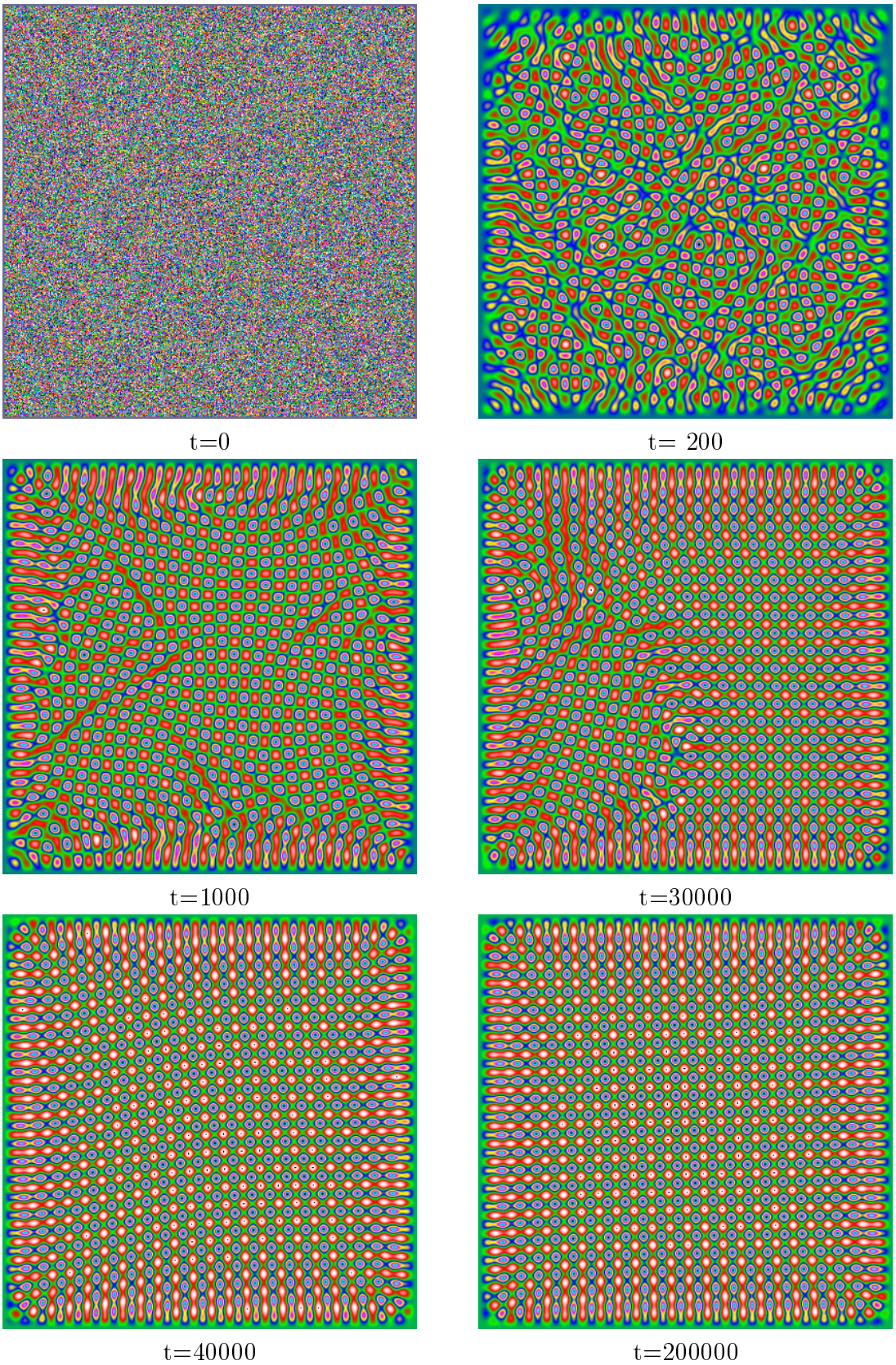

Figure 2: The time evolution of a pattern obtained by numerical simulation of Eq. (2) towards a time-independent tesselation of squares. All defects disappear before $t = 40000$. From this time to the end of the simulation the pattern slowly turns to allign with the sidewalls of the box. Here $\mu = 2.0$, $\alpha = -0.9$, $\beta = \delta = -3\sqrt{7}$, $\gamma = 0$ and $\kappa = -1$.

increment typical of explicit methods, while keeping memory storage requirements at a level quite comparable to the one of explicit methods. We also presented a figure to monitoring the rate of evolution of the pattern which proved to be an usefull tool to decide when to proceed or not with a numerical simulation.

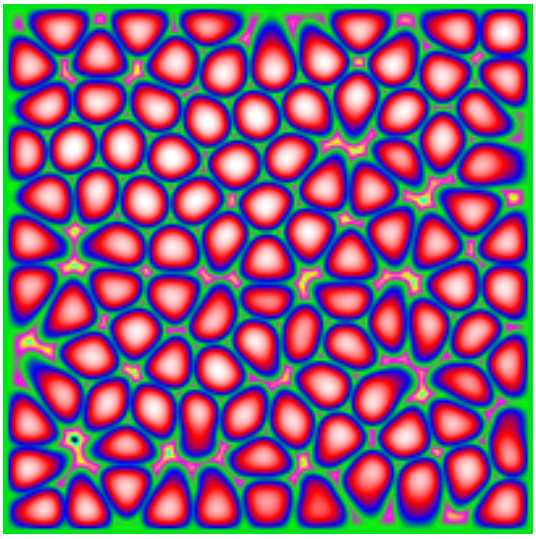

Figure 3: Time dependent pattern obtained by integration of Eq. (2). Here, the coefficients were set to $\mu = 2.0$, $\alpha = -0.3$, $\beta = -0.125\sqrt{7}$, $\delta = 0.75\sqrt{7}$, $\gamma = 0$, $\kappa = -1$, and $\tau_0 = 1$.

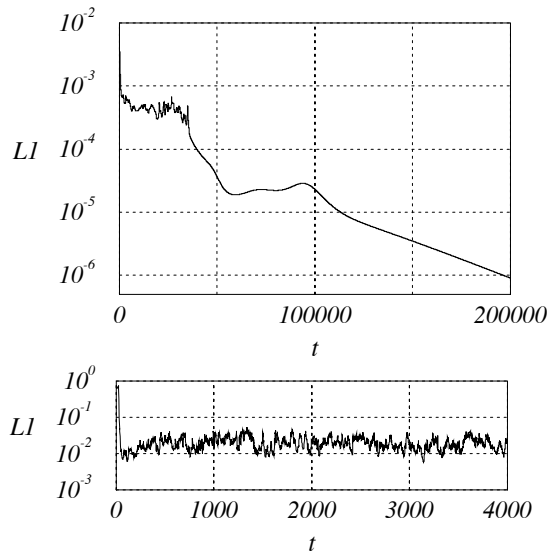

Figure 4: The $L_1 \times t$ curve associated to the evolution shown in Fig. 2 (top) and to the asymptotic time-dependent configuration shown in Fig. 3 (bottom).

References

[1] C. I. Christov, J. Pontes, D. Walgraef, and M. G. Velarde. Implicit time splitting for fourth-order parabolic equations. *Comp. Meth. Appl. Mech. and Eng.*, 1997 (To appear).

[2] J. Douglas and H. H. Rachford. On the numerical solution of heat conduction problems in two and three space variables. *Trans. Amer. Math. Soc.*, 82:421–439, 1956.

[3] E. Knobloch. Pattern selection in long-wavelength convection. *Physica D*, 41:450–479, 1990.

[4] D. W. Peaceman and H. H. Rachford Jr. The numerical solution of paraboloic and eliptic differential equations. *SIAM*, 3:28–41, 1955.

[5] J. Pontes, C. I. Christov, and M. G. Velarde. Numerical study of patterns and their evolution in finite geometries. *Int. J. Bif. & Chaos*, 6,10:1883–1890, 1996.

[6] L. Shtilman and G. Sivashinsky. Hexagonal structure of large-scale Marangoni convection. *Physica D*, 52:477–488, 1991.

[7] J. Swift and P. C. Hohenberg. Hydrodynamic fluctuations at the convective instability. *Phys. Rev. A*, 15:319–328, 1977.

[8] N. N. Yanenko. *Method of Fractional Steps.* Gordon and Breach, NY, 1971.